Design of a MIMO Dielectric Resonator Antenna for LTE Femtocell Base Stations

Jie-Bang Yan, *Member, IEEE*, and Jennifer T. Bernhard, *Fellow, IEEE*

***Abstract*—A novel multiple-input multiple-output (MIMO) dielectric resonator antenna (DRA) for long term evolution (LTE) femtocell base stations is described. The proposed antenna is able to transmit and receive information independently using TE and HE modes in the LTE bands 12 (698–716 MHz, 728–746 MHz) and 17 (704–716 MHz, 734–746 MHz). A systematic design method based on perturbation theory is proposed to induce mode degeneration for MIMO operation. Through perturbing the boundary of the DRA, the amount of energy stored by a specific mode is changed as well as the resonant frequency of that mode. Hence, by introducing an adequate boundary perturbation, the TE and HE modes of the DRA will resonate at the same frequency and share a common impedance bandwidth. The simulated mutual coupling between the modes was as low as -40 dB. It was estimated that in a rich scattering environment with an Signal-to-Noise Ratio (SNR) of 20 dB per receiver branch, the proposed MIMO DRA was able to achieve a channel capacity of 11.1 b/s/Hz (as compared to theoretical maximum 2×2 capacity of 13.4 b/s/Hz). Our experimental measurements successfully demonstrated the design methodology proposed in this work.**

***Index Terms*—Dielectric resonator antenna (DRA), long term evolution (LTE), multiple-input multiple-output (MIMO) antenna, mutual coupling, perturbation method.**

I. Introduction

THE Federal Communications Commission (FCC) recently released the 700 MHz spectrum which was previously used for analog television broadcasting [1]. A new nationwide wireless broadband network based on long term evolution (LTE) technology has been proposed to operate in the 700 MHz spectrum [2], [3]. In the LTE Evolved UMTS terrestrial radio access (E-UTRA) air interface, multiple-input multiple-output (MIMO) technology plays an important role in increasing the system's spectral efficiency [4], [5]. Given the lower operating frequency of the LTE system, as compared to the WiFi and cellular standards, the antenna in handheld devices such as a smartphone or a netbook must be electrically small. This implies the mobile antennas are likely to be inefficient and the coverage of the system is therefore limited. This is especially true if MIMO operation is needed at both mobile and base station since the antenna efficiency would be further reduced due to strong mutual coupling between closely-packed mobile antennas. In view of this, LTE architecture includes a femtocell solution for coverage extension [6]. Femtocells can be considered as low-power access points serving indoor areas. To exploit the richness in multipath propagation in indoor scenarios, it is desired to employ MIMO antennas with a very low mutual coupling as the base station antenna in a femtocell. One possible solution would be the orthogonally polarized MIMO antennas proposed in [7]. However the problem is that such antennas would be oversized when scaled to operate at 700 MHz. Hence, a new MIMO antenna solution for LTE's femtocell base station is necessary.

In this work, a 700 MHz dual-mode MIMO dielectric resonator antenna (DRA) that is suitable for the new wireless system is proposed. Although the cost of DRAs may be high as compared to traditional PIFAs or microstrip antennas, they have the advantages of compact size, high radiation efficiency, and wide impedance bandwidth [8]. Another important feature of DRAs is that the three dimensional structure offers more degrees of freedom in exciting various orthogonal resonant modes, and each mode can be utilized to transmit and receive information independently. This makes the DRA an ideal candidate for application in MIMO communication systems. Indeed, a multi-mode usage of a single dielectric resonator has been suggested in [9], but the emphasis is not on MIMO applications.

The concept of a MIMO DRA was first described and demonstrated by Ishimiya *et al.* in [10], [11]. It was experimentally shown that a cubic MIMO DRA is able to achieve a diversity gain of about 10 dB and has comparable performance to traditional MIMO dipole arrays in practical IEEE 802.11n systems. Nevertheless, in Ishimiya's papers, no explicit design method has been described. The major difficulty of applying DRAs in MIMO systems is to make various modes to resonate at the same frequency while maintaining low coupling between the modes. Here, we introduce a systematic design method for MIMO DRAs. The key in MIMO DRA design is to induce degenerate modes (i.e., modes that have the same resonant frequency). Conventionally, only DRAs that exhibit symmetry can support degenerate modes [12] and this limits any further size reduction of MIMO DRAs. Hence, a novel mode degeneration method based on boundary perturbation is proposed and demonstrated in this work.

Section II describes the base design for the proposed MIMO DRA, then, Section III introduces the boundary perturbation for

Manuscript received May 27, 2010; revised December 14, 2010; accepted February 05, 2011. Date of publication October 28, 2011; date of current version February 03, 2012. This work was supported by the Motorola Center for Communications at the University of Illinois at Urbana-Champaign and a Croucher Foundation Scholarship.

J.-B. Yan was with the Electromagnetics Laboratory, Department of Electrical and Computer Engineering, University of Illinois at Urbana-Champaign, Urbana, IL 61801 USA. He is now with the Center for Remote Sensing of Ice Sheets (CReSIS), University of Kansas, Lawrence, KS 66045 USA.

J. T. Bernhard is with the Electromagnetics Laboratory, Department of Electrical and Computer Engineering, University of Illinois at Urbana-Champaign, Urbana, IL 61801 USA (e-mail: jbernhar@illinois.edu).

Color versions of one or more of the figures in this paper are available online at http://ieeexplore.ieee.org.

Digital Object Identifier 10.1109/TAP.2011.2174021

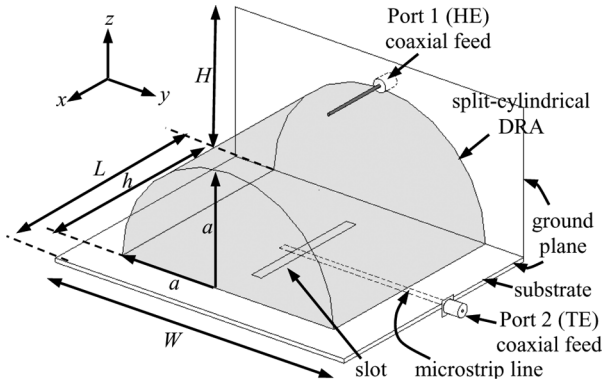

Fig. 1. Perspective view of the split-cylindrical DRA ($a = 44$ mm, $h = 80$ mm, $W = 120$ mm, $L = 95$ mm, and $H = 47.5$ mm).

mode degeneration. In Section IV, we evaluate the performance of the perturbed antenna structure. Simulated results including those for MIMO capacity are provided. Following that, some experimental results are given in Section V as a validation to the developed design methodology. Finally a conclusion and a discussion of future work are given in Section VI.

II. Base Design

Consider a split-cylindrical DRA ($\varepsilon_r = 18$), with a radius a of 44 mm and a length h of 80 mm residing on a ground plane with dimensions as shown in Fig. 1. The $\mathrm{TE}_{011+\delta}$ mode and the $\mathrm{HE}_{11\delta}$ mode can be excited simultaneously using appropriate excitation methods, such as probe feeds, aperture coupling or microstrip feeds. The value of the subscript δ ranges between zero and one, depending on the method of feeding [12]. Here, a 50 Ω microstrip-fed rectangular slot and a probe feed were chosen to excite the $\mathrm{TE}_{011+\delta}$ and $\mathrm{HE}_{11\delta}$ modes, respectively (see Fig. 1). FR-4 epoxy board ($\varepsilon_r = 4.4$) with thickness of 1.6 mm is used as the substrate of the microstrip line. The dimensions of the slot are 50 mm $\times$ 4 mm and the probe that excites the $\mathrm{HE}_{11\delta}$ mode has a length of 27 mm.

Fig. 2 shows the plots of the theoretical magnetic field distributions for the two modes inside the DRA computed using Wolfram Research Mathematica [13]. It can be seen that $\mathrm{TE}_{011+\delta}$ mode behaves as a magnetic dipole on the x-axis while $\mathrm{HE}_{11\delta}$ mode radiates as a short magnetic dipole oriented along the y-axis. The two modes are therefore orthogonal to each other and should exhibit low mutual coupling. The resonant frequencies of the $\mathrm{TE}_{011+\delta}$ mode and $\mathrm{HE}_{11\delta}$ mode can be derived from the separation equation [8] and are found to be 653 MHz and 520 MHz, respectively,

$$f_r^{TE_{011}} = \frac{c}{2\pi\sqrt{\varepsilon_r}}\sqrt{\left(\frac{\chi_{01}}{a}\right)^2 + \left(\frac{\pi}{2h}\right)^2} \quad (1)$$

$$f_r^{HE_{11\delta}} = \frac{c}{2\pi\sqrt{\varepsilon_r}}\sqrt{\left(\frac{\chi'_{11}}{a}\right)^2 + \left(\frac{\pi}{2h}\right)^2} \quad (2)$$

where c is the speed of light in free space, and χ_{01} and χ'_{11} are the first zeros of the zero-order Bessel function and the derivative of the first-order Bessel function, respectively. A full-wave

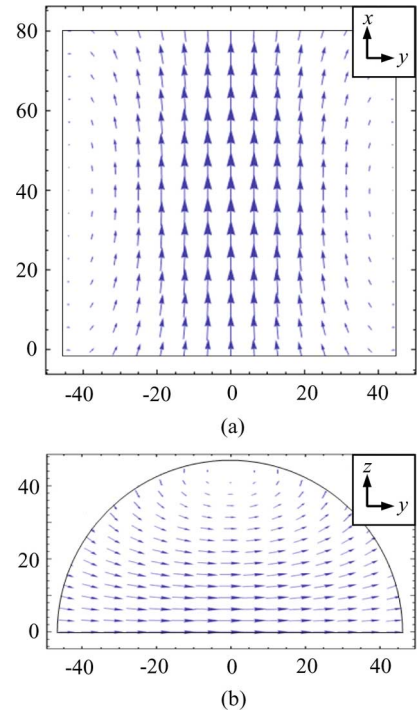

Fig. 2. Theoretical magnetic field distributions for the (a) $\mathrm{TE}_{011+\delta}$ mode, and (b) $\mathrm{HE}_{11\delta}$ mode.

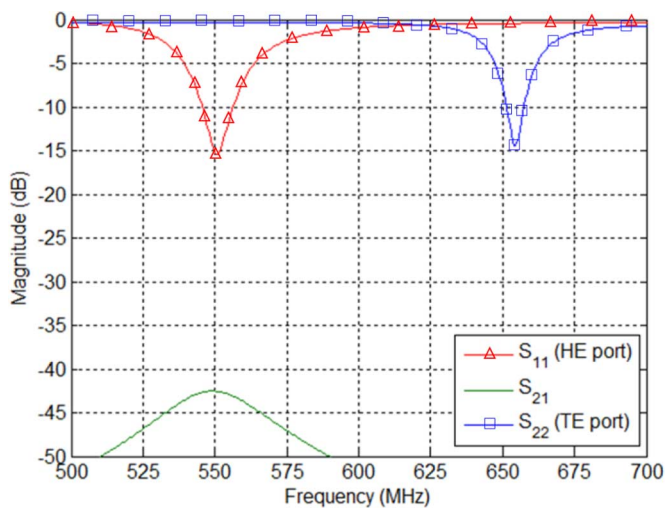

Fig. 3. Simulated S-parameters of the unperturbed cylindrical DRA.

simulation was performed using Ansys HFSS [14] and the simulated S-parameters of the antenna are shown in Fig. 3. The theoretically predicted and simulated operating frequencies of the modes agree very well with each other. It can also be seen that the coupling (S_{21}) between the two modes is very low as expected.

III. Design of MIMO DRA

A. Boundary Perturbation

In order to work in a MIMO system, the two modes should have the same resonant frequency and have a shared impedance bandwidth. To accomplish this, we propose a mode degeneration method based on boundary perturbation. For an arbitrarily

shaped dielectric resonator, the change in resonant frequency due to a change of the cavity wall can be determined using perturbation theory [15], and is given by,

$$\frac{\omega-\omega_0}{\omega_0} \approx \frac{\iiint_{\Delta v}\left(\mu|H_0|^2-\varepsilon|E_0|^2\right)dv}{\iiint_{V}\left(\mu|H_0|^2+\varepsilon|E_0|^2\right)dv} \tag{3}$$

where ε and μ are the permittivity and the permeability of the dielectric resonator respectively, ω and ω_0 are the resonant radian frequencies of the perturbed and unperturbed resonator, respectively, Δv and V are the volume perturbed and the original volume of the resonator, and E_0 and H_0 are the unperturbed fields. Equation (3) indicates that the change in resonant frequency is equal to the electric and magnetic energies removed by the perturbation divided by the total energy stored [15], i.e.,

$$\frac{\omega-\omega_0}{\omega_0} \approx \frac{\Delta\bar{W}_m-\Delta\bar{W}_e}{W} \tag{4}$$

where $\Delta\bar{W}_e$ and $\Delta\bar{W}_m$ are time-averaged electric and magnetic energies originally contained in the volume perturbed (Δv) and W is the total energy stored in the unperturbed cavity.

Now consider a boundary perturbation from the base of the split-cylindrical DRA as depicted in Fig. 4. The changes in resonant frequencies of the $\mathrm{TE}_{011+\delta}$ mode and $\mathrm{HE}_{11\delta}$ mode can be computed using (3), and the result is shown in Fig. 5. It can be observed that as the electric boundary is moved up, the resonant frequency of the $\mathrm{HE}_{11\delta}$ mode increases more rapidly than that of the $\mathrm{TE}_{011+\delta}$ mode. Hence, at a certain perturbation value, the two resonant frequencies should overlap and thus fulfill the primary requirement for MIMO antenna design. According to (4), the difference in the rate of change of resonant frequency can be explained by the difference in the energy stored by the two modes in the perturbation volume Δv. To verify the boundary perturbation method, an HFSS simulation was carried out and the result is also shown in Fig. 5. It can be seen that the result predicted by the boundary perturbation method starts to deviate from the result obtained from HFSS when the perturbation, α, increases. This is due to the substitution of the original fields into the perturbed fields during the derivation of (3). The difference between the original fields and the perturbed fields would be intolerable when the perturbation is too large. Thus, the deviation at large perturbations is inherent in the perturbation analysis. Nonetheless, the boundary perturbation method gives a good initial guess on how much perturbation is required to make the two modes resonate at the same frequency. According to the HFSS simulation result, the two modes both resonate at 700 MHz when the perturbation, α, is 13 mm.

In (3), there is no specific constraint on the geometry of the cavity, hence, the proposed boundary perturbation method can be applied to DRAs of any other shapes with arbitrary perturbations. However, the difficulty of analysis of such structures might be the evaluation of the integrals in (3).

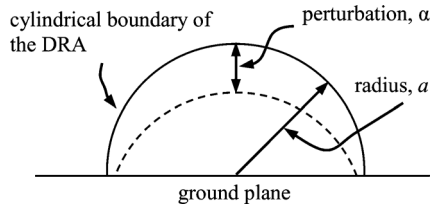

Fig. 4. Boundary perturbation from the base of the split-cylindrical DRA (Cross-sectional (yz-plane) view).

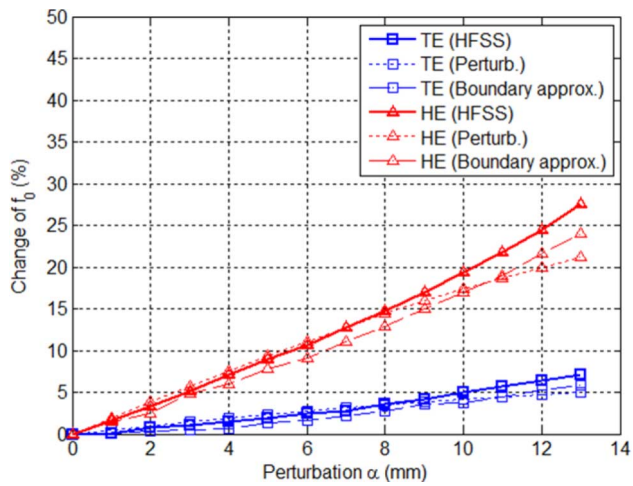

Fig. 5. Plot of change of resonant frequency f_0 against the perturbation parameter α.

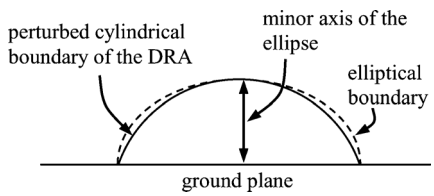

Fig. 6. Elliptical approximation of the perturbed cylindrical boundary (Cross-sectional (yz-plane) view).

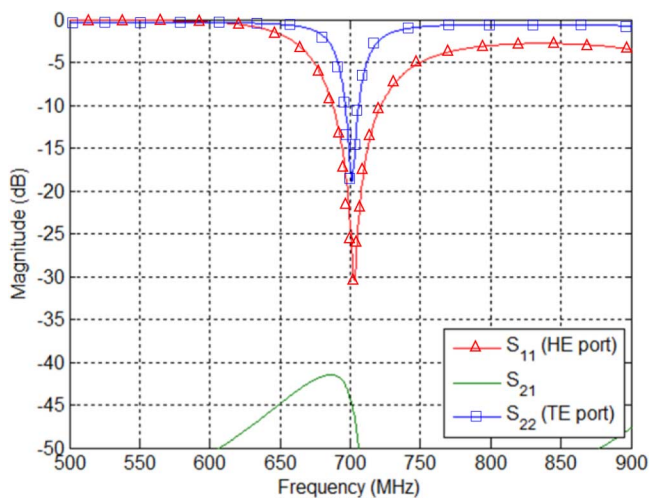

Fig. 7. Simulated S-parameters of the perturbed cylindrical DRA.

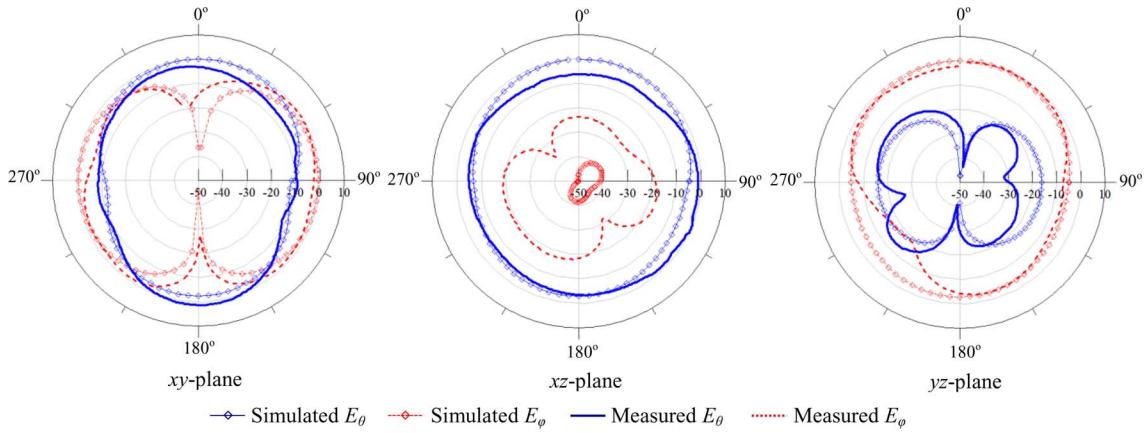

Fig. 8. Comparison of the simulated and measured radiation patterns of Port 1 (HE mode).

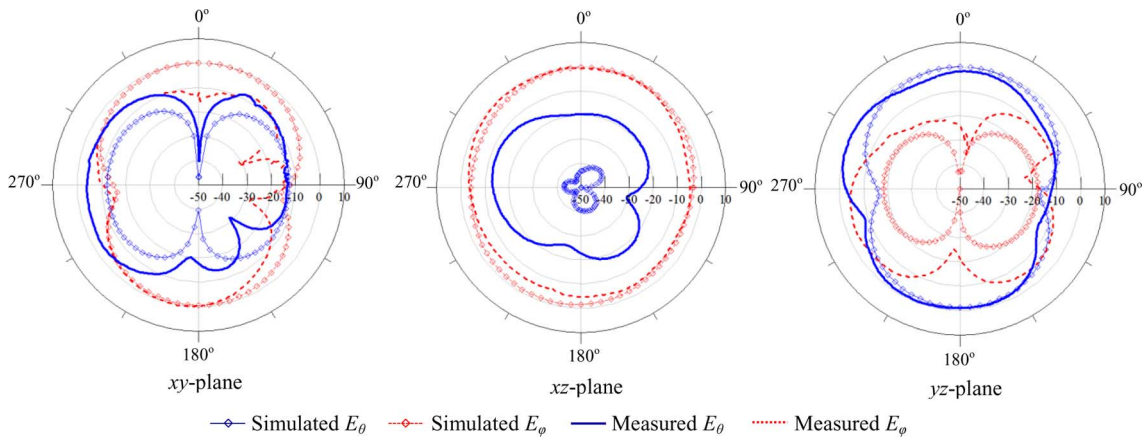

Fig. 9. Comparison of the simulated and measured radiation patterns of Port 2 (TE mode).

B. Boundary Approximation

While the above described boundary perturbation method obtains the solutions by approximating the fields, boundary approximation estimates the change in resonant frequency by approximating the structure of the resonator. According to Fig. 6, a perturbed cylindrical boundary can be modeled by a half ellipse. The accuracy of this method depends on how well the perturbed circular arc is approximated by an elliptic arc. The resonant frequencies of various modes in an elliptical DRA can be found by expanding the fields inside the cavity in Mathieu functions and applying the technique of separation of variables. A detailed analysis of an elliptical DRA can be found in [16]. The resonant frequencies of a series of split-elliptical DRAs of various minor axes, which corresponded to the previously described set of perturbed cylindrical DRAs, are computed, and the change in resonant frequency estimated by this boundary approximation method is plotted in Fig. 5. The results obtained agree very well with those calculated by both the boundary perturbation method and full-wave simulations.

IV. Simulated Antenna Performance

A. Antenna Characteristics

From Section III-A, the $\mathrm{TE}_{011+\delta}$ mode and the $\mathrm{HE}_{11\delta}$ mode of a split-cylindrical DRA will both resonate at 700 MHz when the perturbation, α, is 13 mm. The dimensions of the perturbed DRA are 80 mm $\times$ 84 mm $\times$ 31 mm. Given the same resonant frequency and a half-wavelength antenna separation, the dimensions of a two-element MIMO PIFA would be 107 mm $\times$ 214 mm $\times$ 5 mm. Since coupling between antenna ports is another important parameter to characterize MIMO antennas, the proposed antenna structure was simulated in HFSS. The simulated S-parameters of the antenna were obtained with 50 Ω terminations at both ports and are given in Fig. 7. It can be observed that the mutual coupling between the two modes is insensitive to the perturbation (see Fig. 3) and is less than -40 dB. This is significantly lower than the mutual coupling in conventional MIMO antennas that are based on dipole antennas, patch antennas or PIFAs [17]–[20]. The impedance bandwidths (defined as $|S_{11}| < -9.8$ dB) of the $\mathrm{TE}_{011+\delta}$ mode and the $\mathrm{HE}_{11\delta}$ mode are 10 MHz and 35 MHz respectively. The $\mathrm{TE}_{011+\delta}$ mode has a relatively narrow bandwidth and limits the overall bandwidth of the antenna. Nevertheless, the bandwidth of the $\mathrm{TE}_{011+\delta}$ mode can be improved using well known bandwidth broadening techniques, such as inserting an air gap between the ground plane and the DRA [21], [22], or adding a matching stub at the end of the microstrip line [23]. The simulated gains of the $\mathrm{TE}_{011+\delta}$ and $\mathrm{HE}_{11\delta}$ modes are 3.96 and 3.19 dBi, respectively. The simulated radiation patterns of the two modes, which are orthogonal to each other, are given in Figs. 8 and 9. Hence, the antenna is

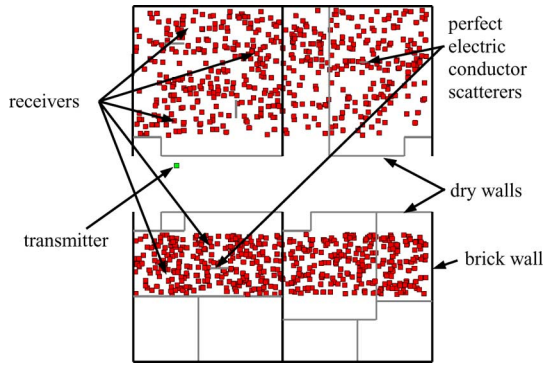

Fig. 10. The floor plan (16 m × 19 m) of the office environment that was used to estimate the MIMO channel capacity (notice that there is no line-of-sight (LOS) path between the transmitter and any of the receivers).

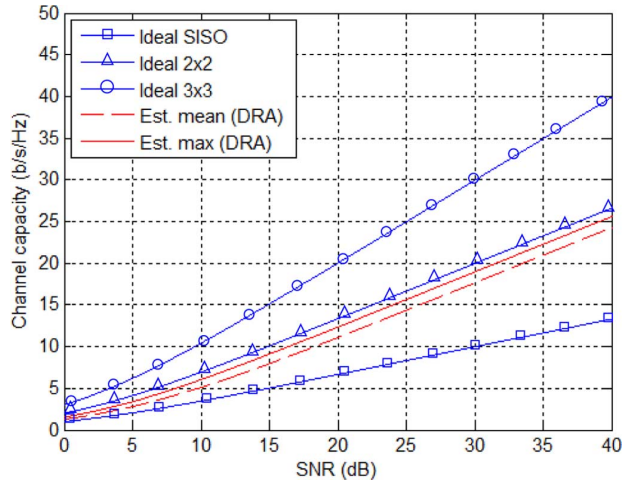

Fig. 11. Estimated channel capacity of the proposed MIMO DRA.

able to exploit polarization diversity and the pattern orthogonality leads to low mutual coupling between the ports.

B. MIMO Performance Evaluation

The channel capacity gain by using the proposed antenna was evaluated with the aid of Remcom Wireless Insite [24]. In the simulation setup, a single transmitter and 1000 identical receivers were placed in an office environment as shown in Fig. 10. The office environment was constructed to resemble a rich scattering environment (i.e., the channel statistics are approximately Rayleigh distributed). In order to resemble a time-varying MIMO channel, the receivers were randomly spread across the designated area of the office such that a 1000 non-line-of-sight (NLOS) communication links were established. In all the simulations, there were 80 paths for each channel realization. The simulated complex radiation patterns (including both polarizations, E_θ and E_φ) of the proposed antennas were used at the transmitter and all the receivers. 1000 samples of the unnormalized channel matrix were then obtained from the simulation [25],

$$H^m = \begin{bmatrix} h_{11}^m & h_{12}^m \\ h_{21}^m & h_{22}^m \end{bmatrix} \tag{5}$$

where there are $m(=1,2,\ldots,1000)$ communication links, and H^m is the unnormalized channel matrix of the m-th link. Here, h_{uv}^m represents the m-th sample of the complex channel gain between port u of the transmitter and port v of the receiver, where subscripts $u=1,2$ and $v=1,2$:

$$h_{uv}^m = \sum_{n=1}^{k_m} \sqrt{P_n^m} e^{j\psi_n^m}. \tag{6}$$

Here k_m is the number of path in the m-th link; P_n^m is the received power contributed by the n-th path in the m-th link; Ψ_n^m is the phase of the n-th path in the m-th link. From the simulated channel data, it was found that the coherence bandwidth of the wireless channel was much larger than the bandwidth of the proposed antenna. Hence, for equal power distributed among the transmit antennas, the flat-fading MIMO channel capacity of the m-th link, C^m, can be calculated by [25]–[27]

$$C^m = \log_2 \left[\det \left(I_{N_r} + \frac{\bar{\rho}}{N_t} H_{norm}^m H_{norm}^{m\dagger} \right) \right] \tag{7}$$

where N_t and N_r denote the number of transmit and receiver antennas, respectively; I_{N_r} is an identity matrix with dimension N_r; $\bar{\rho}$ is the mean signal-to-noise ratio (SNR) per receive branch; $\{\cdot\}^\dagger$ represents a complex conjugate transpose; and H_{norm}^m is the m-th normalized channel matrix

$$H_{norm}^m = \frac{H^m}{\sqrt{\frac{\|H^m\|_F^2}{N_t N_r}}} \tag{8}$$

where $\|\cdot\|_F^2$ denotes a Frobenius norm. The mean capacity and the maximum achievable capacity obtained by using the proposed antenna are plotted in Fig. 11. Fig. 11 also gives the theoretical channel capacities for single-input single-output (SISO), 2×2 and 3×3 channels with zero mean, unity variance, i.i.d. complex Gaussian distributed channel elements for comparison. The results indicate that the estimated mean channel capacity is 11.1 b/s/Hz at an SNR of 20 dB per receiver branch. The maximum achievable capacity is very close to the theoretical maximum 2×2 MIMO capacity of 13.4 b/s/Hz. The small discrepancy between the theoretical and simulated capacities may be due to the non-ideal scattering environment and finite mutual coupling between the modes. Nevertheless, the simulation results reflect the utility of the antenna design, and a prototype antenna is presented in Section V.

V. Measurement Results

The perturbed cylindrical DRA was built and tested in the Electromagnetics Laboratory at University of Illinois at Urbana-Champaign. The dielectric material ($\varepsilon_r = 18$ and loss tangent < 0.00015) was supplied by Countis Laboratories [28]. The dielectric block was bonded onto the ground plane

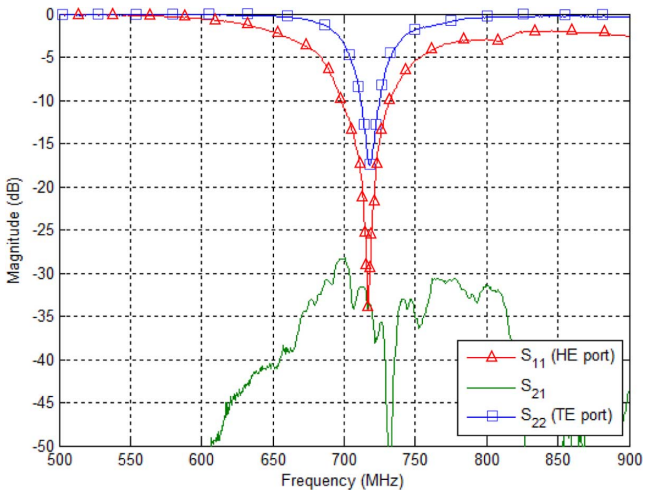

Fig. 12. Measured S-parameters of the perturbed cylindrical DRA.

with silver epoxy so as to prevent any air gaps between the dielectric and ground plane. This is important because for DRAs with high permittivities, air gaps of less than 0.05 mm can be enough to significantly alter the expected input impedance [12]. The S-parameters of the perturbed cylindrical DRA were measured using Agilent's two-port Network Analyzer E8363B (with 50 Ω reference impedance). The measured results are given in Fig. 12, which are very close to the simulated results given in Fig. 7. Both modes are well matched at 717 MHz. The coupling between the ports (S_{21}) is less than -30 dB at the operating frequency. The measured impedance bandwidths of the $\mathrm{TE}_{011+\delta}$ mode and the $\mathrm{HE}_{11\delta}$ mode are 13.5 MHz and 35 MHz, respectively. The measured radiation patterns along the three principal cuts are given in Figs. 8 and 9. Despite a small distortion of the pattern at some angles, the measured patterns agreed reasonably well with the simulated ones. The complementary nature of the two orthogonal modes can still be observed clearly.

VI. Conclusion

A 2-port MIMO antenna based on a split-cylindrical DRA is described in this work. A mode degeneration method derived from perturbation theory is proposed to make the TE and HE modes of the split-cylindrical DRA resonate at the same frequency. The proposed method has been verified by both full-wave simulations and the boundary (elliptical) approximation method, and can be applied to DRAs of any shape. The fabricated MIMO DRA was tested and the experimental results show very good agreement with the simulated results. Indeed, given that the same operating frequency and the same dielectric material, the antenna described in this paper is smaller in volume, has lower profile, has a smaller ground plane and has much lower mutual coupling as compared to the work in [10], [11]. The proposed antenna is potentially suitable as the femtocell base station antenna in the forthcoming nationwide mobile broadband system based on LTE technology. Future work related to this paper will be a frequency reconfigurable MIMO DRA which can easily be adapted to other LTE bands and other wireless standards.

References

[1] Federal Communications Commission, "700 MHz band," Auction 73 Feb. 2009.
[2] News Archives AT&T Inc., 2008 [Online]. Available: http://www.att.com/
[3] News Archives Verizon Wireless, 2009 [Online]. Available: http://news.vzw.com/
[4] 3GPP TS36.300, "Evolved Universal Terrestrial Radio Access (E-UTRA) and Evolved Universal Terrestrial Radio Access Network (E-URRAN): Overall Description,".
[5] D. Astely, E. Dahlman, A. Furuskar, Y. Jading, M. Lindstrom, and S. Parkvall, "LTE: The evolution of mobile broadband—[LTE part II: 3GPP release 8]," *IEEE Commun. Mag.*, vol. 47, no. 4, pp. 44–51, Apr. 2009.
[6] V. Chandrasekhar and J. Andrews, "Femtocell networks: A survey," *IEEE Commun. Mag.*, vol. 46, no. 9, pp. 59–67, Sep. 2008.
[7] C.-Y. Chiu, J.-B. Yan, and R. D. Murch, "Compact three-port orthogonally polarized MIMO antennas," *IEEE Antennas Wireless Propag. Lett.*, vol. 6, pp. 619–622, 2007.
[8] K.-M. Luk and K.-W. Leung, *Dielectric Resonator Antennas*. Hertfordshire, England: Research Studies Press Ltd., 2003.
[9] L. K. Hady, D. Kajfez, and A. A. Kishk, "Triple mode use of a single dielectric resonator," *IEEE Trans. Antennas Propag.*, vol. 57, no. 5, pp. 1328–1335, May 2009.
[10] K. Ishimiya, J. Langbacka, Z. Ying, and J.-I. Takada, "A compact MIMO DRA antenna," in *Proc. IEEE Int. Workshop on Antenna Technology: Small Antennas and Novel Metamaterials (IWAT '08)*, Chiba, Japan, Mar. 2008, pp. 286–289.
[11] K. Ishimiya, Z. Ying, and J.-I. Takada, "A compact MIMO DRA for 802.11n application," presented at the IEEE Antennas and Propagation Society Int. Symp., San Diego, CA, Jul. 2008.
[12] A. Petosa, *Dielectric Resonator Antenna Handbook*. Norwood, MA: Artech House, 2007.
[13] *Mathematica,* Wolfram Research Inc., 2010.
[14] *HFSS* Ansys, Inc., 2010.
[15] R. F. Harrington, *Time-Harmonic Electromagnetic Fields*. New York: IEEE Press, 2001.
[16] A. Tadjalli and A. Sebak, "Resonance frequencies and far field patterns of elliptical dielectric resonator antenna: Analytical approach," in *Progress in Electromagnetic Research, PIER 64*, 2006, pp. 81–98.
[17] C.-C. Hsu, K. H. Lin, H.-L. Su, H.-H. Lin, and C.-Y. Wu, "Design of MIMO antennas with strong isolation for portable applications," presented at the IEEE Antennas and Propagation Society Int. Symp., Charleston, SC, Jun. 2009.
[18] H. Zhang, Z. Wang, J. Yu, and J. Huang, "A compact MIMO antenna for wireless communication," *IEEE Antennas Propag. Mag.*, vol. 50, no. 6, pp. 104–107, Dec. 2008.
[19] K.-S. Min, D.-J. Kim, and M.-S. Kim, "Multi-channel MIMO antenna design for WiBro/PCS band," in *Proc. IEEE Antennas and Propagation Society Int. Symp.*, Hawaii, Jun. 2007, pp. 1225–1228.
[20] K. Chung and J. H. Yoon, "Integrated MIMO antenna with high isolation characteristics," *Electron. Lett.*, vol. 43, no. 4, pp. 199–201, Feb. 2007.
[21] M. Cooper, "Investigation of Current and Novel Rectangular Dielectric Resonator Antennas for Broadband Applications at L-band Frequencies," M.Sc. thesis, Carleton University, Ottawa, ON, Canada, 1997.
[22] S.-M. Deng, C.-L. Tsai, S.-F. Chang, and S.-S. Bor, "A CPW-fed suspended, low profile rectangular dielectric resonator antenna for wideband operation," in *Proc. IEEE Antennas and Propagation Society Int. Symp.*, Washington, D.C., Jul. 2005, vol. 4B, pp. 242–245.
[23] P. V. Bijumon, S. K. Menon, M. N. Suma, M. T. Sebastian, and P. Mohanan, "Broadband cylindrical dielectric resonator antenna excited by modified microstrip line," *Electron. Lett.*, vol. 41, no. 7, pp. 385–387, Mar. 2005.
[24] *Wireless Insite,* Remcom Inc., 2006.
[25] J. D. Boerman and J. T. Bernhard, "Performance study of pattern reconfigurable antennas in MIMO communication systems," *IEEE Trans. Antennas Propag.*, vol. 56, no. 1, pp. 231–236, Jan. 2008.
[26] G. J. Foschini and M. J. Gans, "On limits of wireless communications in a fading environment when using multiple antennas," in *Wireless Personal Commun.*. New York: Kluwer Academic Press, 1998, pp. 311–335.
[27] Z. Tang and A. S. Mohan, "Experimental investigation of indoor MIMO Ricean channel capacity," *IEEE Antennas Wireless Propag. Lett.*, vol. 4, pp. 55–58, 2005.
[28] Countis Laboratories [Online]. Available: http://www.countis.com/

Jie-Bang Yan (S'09–M'11) received the B.Eng. degree (first class honors) in electronic and communications engineering from the University of Hong Kong, in 2006, the M.Phil. degree in electronic and computer engineering from the Hong Kong University of Science and Technology, in 2008, and the Ph.D. degree in electrical and computer engineering from the University of Illinois at Urbana-Champaign, in 2011.

He was a Croucher Scholar from 2009 to 2011 while he did his Ph.D. at the University of Illinois at Urbana-Champaign. Upon graduation, he joined the Center for Remote Sensing of Ice Sheets (CReSIS), University of Kansas, where he is currently an Assistant Research Professor. His research interests include design and analysis of MIMO and reconfigurable antennas, RF propagation, radar antenna designs, and fabrication of on-chip antennas. He holds two U.S. patents and a U.S. patent application related to novel antenna technologies.

Dr. Yan was the recipient of the Best Paper Award at the 2007 IEEE (HK) AP/MTT Postgraduate Conference and the 2011 Raj Mittra Outstanding Research Award at Illinois. He serves as a Reviewer for several journals and conferences on antennas and electromagnetics.

Jennifer T. Bernhard (S'89–M'95–SM'01–F'10) was born on May 1, 1966, in New Hartford, NY. She received the B.S.E.E. degree from Cornell University, Ithaca, NY, in 1988 and the M.S. and Ph.D. degrees in electrical engineering from Duke University, Durham, NC, in 1990 and 1994, respectively, with support from a National Science Foundation Graduate Fellowship.

While at Cornell, she was a McMullen Dean's Scholar and participated in the Engineering Co-op Program, working at IBM Federal Systems Division in Owego, New York. During the 1994–95 academic year she held the position of Postdoctoral Research Associate with the Departments of Radiation Oncology and Electrical Engineering at Duke University, where she developed RF and microwave circuitry for simultaneous hyperthermia (treatment of cancer with microwaves) and MRI (magnetic resonance imaging) thermometry. From 1995–1999, she was an Assistant Professor in the Department of Electrical and Computer Engineering, University of New Hampshire, where she held the Class of 1944 Professorship. Since 1999, she has been with the Electromagnetics Laboratory, Department of Electrical and Computer Engineering, University of Illinois at Urbana-Champaign, where she is now a Professor. Her industrial experience includes work as a Research Engineer with Avnet Development Labs and, more recently, as a private consultant for members of the wireless communication and sensors community. Her research interests include reconfigurable and wideband microwave antennas and circuits, wireless sensors and sensor networks, high speed wireless data communication, electromagnetic compatibility, and electromagnetics for industrial, agricultural, and medical applications, and has four patents on technology in these areas.

Prof. Bernhard is a member of URSI Commissions B and D, Tau Beta Pi, Eta Kappa Nu, Sigma Xi, and ASEE. She is a Fellow of the IEEE. She was an organizing member of the Women in Science and Engineering (WISE) Project at Duke, a graduate student-run organization designed to improve the climate for graduate women in engineering and the sciences. In 1999 and 2000, she was a NASA-ASEE Summer Faculty Fellow at the NASA Glenn Research Center, Cleveland, OH. She received the NSF CAREER Award in 2000. She is also an Illinois College of Engineering Willett Faculty Scholar and a Research Professor in Illinois' Coordinated Science Laboratory, and the Information Trust Institute. She and her students received the 2004 H. A. Wheeler Applications Prize Paper Award from the IEEE Antenna and Propagation Society for their paper published in the March 2003 issue of the IEEE TRANSACTIONS ON ANTENNAS AND PROPAGATION. She served as an Associate Editor for the IEEE TRANSACTIONS ON ANTENNAS AND PROPAGATION from 2001–2007 and for *IEEE Antennas and Wireless Propagation Letters* from 2001–2005. She is also a member of the editorial board of *Smart Structures and Systems*. She served as an elected member of the IEEE Antennas and Propagation Society's Administrative Committee from 2004–2006. She was President of the IEEE Antennas and Propagation Society in 2008.